



# Characterization of progressive changes in pedicle morphometry and neurovascular anatomy during growth in adolescent idiopathic scoliosis versus adolescents without scoliosis

Colin M. Davis<sup>1,2</sup> · Caroline A. Grant<sup>1</sup> · Maree T. Izatt<sup>1</sup> · Geoffrey N. Askin<sup>1,2</sup> · Robert D. Labrom<sup>1,2</sup> · Clayton J. Adam<sup>1</sup> · Mark J. Pearcy<sup>1</sup> · J. Paige Little<sup>1</sup>

Received: 26 March 2020 / Accepted: 8 June 2020 / Published online: 17 June 2020  
© Scoliosis Research Society 2020

## Abstract

**Study design** Prospective cohort study.

**Objectives** Investigate the progressive changes in pedicle morphometry and the spatial relationship between the pedicles and neurovascular structures in patients with AIS during growth.

**Summary of background data** Adolescent idiopathic scoliosis (AIS) is a complex three-dimensional spine deformity. AIS pedicles are known to be asymmetrical when compared to adolescents without scoliosis. Defining the anatomical changes occurring progressively in scoliosis as it increases with time and growth is essential for understanding the pathophysiology of scoliosis and for treatment planning. MRI is the ideal method to study the growing spine without ionising radiation.

**Methods** 24 females with AIS (mean 12.6 years, right sided main thoracic curves) and 20 non-scoliotic females (mean 11.5 years) were selected from an ongoing database. Participants underwent two 3D MRI scans (3 T scanner, T1, 0.5 mm isotropic voxels) approximately 1 year apart (AIS: mean  $1.3 \pm 0.05$  years, control: mean  $1.0 \pm 0.1$  years). The pedicle width, chord length, pedicle height, transverse pedicle angle, sagittal pedicle angle, distance from vertebrae to aorta and distance from pedicle to dural sac were measured from T5 to T12. Inter- and intra-observer variability was assessed.

**Results** From scans 1–2 in the AIS group, the dural sac became closer to the left pedicle ( $p < 0.05$ , T6, T8–T10 and T12) while the distance from the vertebrae to the aorta increased ( $p < 0.05$ , T6–T10). No significant changes in these measurements were observed in the non-scoliotic group. Between scans, the AIS chord length and transverse pedicle angle increased on the left side around the apex ( $p < 0.05$ ) creating asymmetries not seen in the non-scoliotic cohort. The mean pedicle height increased symmetrically in the non-scoliosis cohort ( $p < 0.05$ ) and asymmetrically in the AIS group with the right side growing faster than the left at T6–T7 ( $p < 0.05$ ).

**Conclusion** Asymmetrical growth patterns occur in the vertebral posterior elements of AIS patients compared to the symmetrical growth patterns found in the non-scoliotic participants.

**Level of evidence** Level II prospective comparative study.

**Keywords** Adolescent idiopathic scoliosis (AIS) · Magnetic resonance imaging · Scoliosis · Spine deformity · Pedicle height · Posterior elements · Asymmetrical growth

## Introduction

Adolescent idiopathic scoliosis (AIS) is the most prevalent three-dimensional spine deformity, affecting 2–3% of children aged between 10 and 16 years with females having up to a tenfold greater risk of curve progression [1, 2]. While this condition does not increase patient mortality, if left untreated, the curve may progress resulting in abnormal posture, increased back pain, body image issues, depression and in extreme conditions, pulmonary symptoms for

✉ J. Paige Little  
j2.little@qut.edu.au

<sup>1</sup> Biomechanics and Spine Research Group, Institute of Health and Biomedical Innovation at Centre for Children's Health Research, Queensland University of Technology and Mater Health Services, Level 5, 62 Graham Street, South Brisbane, QLD 4101, Australia

<sup>2</sup> Queensland Children's Hospital, Brisbane, Australia

those with large thoracic curves [3]. The exact aetiology is unknown but postulated to be multifactorial with genetic predisposition [4].

Operative treatment is usually reserved for patients with major curve angles greater than 45°, with evidence supporting curves 50° or larger will continue to progress even after skeletal maturity [3]. Instrumented surgical fusion using multiple pedicle screws via a posterior approach is a widely used technique to correct and stabilise progressive scoliosis. Understanding the asymmetrical features of scoliotic vertebral morphology and the relationships to surrounding neurovascular structures in the thoracic and lumbar spine is essential for pedicle screw placement as misplacement can potentially cause serious neurologic, vascular or visceral injury [5–10].

To date, numerous studies have assessed the pedicle morphology of AIS spines using a variety of measurements and modalities, and have found asymmetries at the apex of the scoliosis [11–18]. But exposing children and adolescents to a single or repeated CT scans or radiographs involves doses of ionising radiation which should be minimised or avoided in this population. Smaller pedicle widths and heights on the concave side of the scoliotic curve were reported, and two studies also found asymmetrical pedicle orientations in the transverse and sagittal planes [11, 19]. Limitations with all the prior studies are that the cohorts assessed were of mixed skeletal maturity, had significant curves awaiting surgical correction and were analysed at a single point in time. Additionally, with no control subjects in these studies, there was an assumption made that non-scoliotic adolescents had anatomical symmetry and grew symmetrically throughout growth.

This study aims to look at the growing spine in both AIS and non-scoliotic healthy spine subjects using sequential MRI scans to quantify any asymmetries that occur over time in the pedicles as well as the relationships of the vertebrae to the surrounding dural sac and aorta.

## Methods

Magnetic resonance imaging (MRI) scans of the thoracolumbar spine of 24 AIS patients and 20 non-scoliotic participants were selected from an ongoing database of scans for a larger study. Ethical approval for this project was granted by both the Hospital and University Ethics Committees at the authors' institutions.

The inclusion criteria for the clinically diagnosed AIS patients were as follows: (1) female aged 10–16 years with a Risser grade [20] of 0, 1 or 2 for the first scan; (2) right-sided major thoracic curve; (3) MRI scans of a sufficient quality such that they were not affected by patient movement artefact; (4) have undergone two MRI scans at least 5 months apart. All scoliosis curve measurements were performed by two highly experienced spine orthopaedic surgeons (authors GNA and RDL).

The inclusion criteria for the non-scoliotic adolescents were as follows: (1) female aged 10–12 years for their first scan; (2) premenarchal or onset of menarche less than 1 year previously, (3) no personal or family history of scoliosis or serious spine disorders; (4) no clinical signs of scoliosis in standing, and no trunk/ribcage asymmetry found with Adams' Forward Bend Test; (5) had undergone two MRI scans at least 5 months apart. As there were no radiographs available for the non-scoliotic adolescents, the date of menarche and the change in standing height between scans were used as indicators of skeletal maturity in individuals. Assessment for clinical signs of scoliosis or trunk/ribcage asymmetry was determined by a highly experienced spine physiotherapist (author MTI). Cohort demographics are given in Table 1.

### MRI scanning protocol

High-resolution 3D MRI scans were obtained using a 3 Tesla (3 T) scanner (Philips Achieva 3.0 T TX Dual

**Table 1** Demographics of study patients

	AIS patients	Non-scoliotic controls
Number of subjects ( <i>n</i> )	24	20
Mean age at 1st scan (years)	12.6 ± 1.4	11.5 ± 0.8
Mean age at 2nd scan (years)	14.0 ± 1.4	12.5 ± 0.8
Number of subjects premenarchal at 1st scan	16	16
Mean months since menarche at 1st scan (months)	4.7 ± 3.7 ( <i>n</i> = 8)	4.3 ± 4.6 ( <i>n</i> = 4)
Mean interval between 1st and 2nd scan (years)	1.29 ± 0.6	1.0 ± 0.1
Mean major Cobb angle at 1st scan (°)	31.5 ± 10.7	–
Mean major Cobb angle at 2nd scan (°)	44.0 ± 15.3	–
Number of spinal levels in major curve	7.3 ± 1.0	–
Standing height increase scans 1–2 (cm)	6.0 ± 4.8	6.4 ± 2.4

Values are presented as mean ± standard deviation

Transit system, Amsterdam, Netherlands) with the sequence being a T1-weighted 3D gradient echo sequence, TR = 5.9 ms, TE = 2.7 ms, flip angle = 5°, voxel size of 0.5 × 0.5 × 0.5 mm). For the AIS patients, the entire major curve was captured. For the non-scoliotic participants, the most cranial slice was positioned at the mid-height of the T3 vertebra and the most caudal slice was usually at L1 (due to an acquisition window size of 250 × 250 × 95 mm), and depending on the height of the subject.

### Image processing

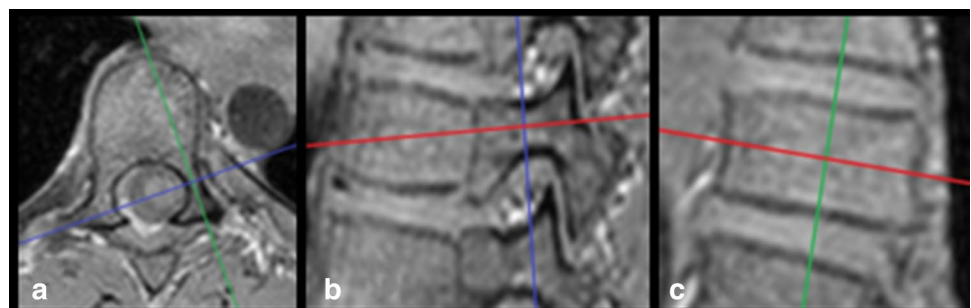
The MRI scans were processed using AMIRA 5.50 (FEI, Hillsboro, OR, USA). Synchronised coronal, axial and sagittal slices were displayed with contrast levels adjusted to enable clear bone and soft tissue demarcation.

The pedicles on both sides of each vertebra were measured using the protocol of a previous CT-based study [11]. The local axial viewing plane (Fig. 1a) was aligned with the pedicle axis (red line in Fig. 1b) and parallel to the superior and inferior endplates of the selected vertebrae (red line in Fig. 1c). Where the superior and inferior endplates were not parallel, an angulation bisecting the two endplate inclinations was used. The local sagittal viewing plane (Fig. 1a) was then aligned with the pedicle axis and perpendicular to the local axial plane (green line in Fig. 1a).

### Measurement of anatomic landmarks

Anatomical landmarks were identified and measured on each pedicle (Table 2) of all vertebrae from T5 to T12 in both cohorts, using measurement definitions from previous studies [11, 12, 19]. A small number of the major curves extended into T4 ( $n=2$ ) and/or L1 ( $n=2$ ) but due to the small numbers with these curve limits, these measurements were excluded from the analysis. After identifying the 3D coordinates of 30 points on each vertebra, the distances and angles were calculated for the following parameters: pedicle width (PW), chord length (CL), transverse pedicle angle (TPA), pedicle height (PH), sagittal pedicle angle (SPA), distance from pedicle to dural sac, and distance from vertebrae to aorta.

**Fig. 1** **a** Local axial viewing plane with sagittal slice (green line) in line with pedicle axis; **b** local sagittal viewing plane with axial slice (red line) in line with pedicle axis; **c** local coronal viewing plane with axial slice (red line) approximately parallel to superior and inferior endplates



### Statistical analysis

To assess measurement variability, three AIS scans (totaling 36 pedicles) with marked vertebral distortion and asymmetry were selected and re-measured 4 months later to calculate the intra-observer variability. The same three scans were measured by a fellow researcher to assess the inter-observer measurement variability. AIS scans which had marked asymmetries were selected for this analysis as it was considered that these scans would likely result in the highest inter- and intra-observer measurement variability. The 95% limits of agreement, as proposed by Bland and Altman were calculated [21].

The Wilcoxon matched-pairs-signed-rank test ( $p < 0.05$ ) was used as a Shapiro–Wilk test indicated the samples did not follow a normal distribution (SPSS Version 22.0, IBM Corp, Armonk, NY, USA).

In the AIS and non-scoliotic subject measurements, the differences between the left and right sides from the first to the second scan were compared. The vertebral growth patterns and temporal change in position of the surrounding neurovascular structures were compared.

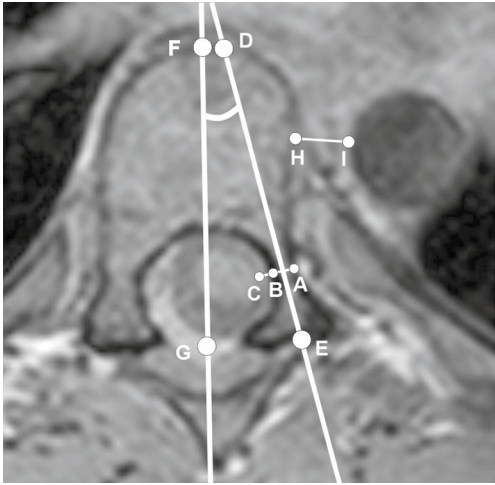
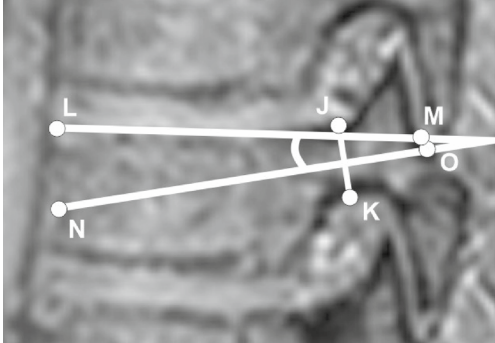
Regression analysis compared mean change in anatomical measurements with vertical height change and major curve angle change between the first and second scans.

### Results

#### Inter- and intra-observer measurement variability

The inter- and intra-observer measurement variability (95% limits of agreement) was found to be lower for linear measurements than the angular measurements (Table 3). The intra-observer variability was lower than the inter-observer error in most cases.

**Table 2** A: An example axial MRI image illustrating the identifying landmarks, lines and angles measured; B: Description of distances and angles measured

2A: MRI Scan of Vertebrae & Points Identified	2B: Measurements Calculated
 <p>A: Left pedicle lateral outer cortical margin            B: Left pedicle medial outer cortical margin            C: Dural Sac margin closest to point B            D: Anterior cortical margin of vertebral body in line with the left pedicle axis            E: Posterior cortical margin of vertebra along in line with the left pedicle axis            F: Anterior cortical margin in line with the sagittal midvertebral line            G: Sagittal midvertebral line at the point of the joining of the two laminae            H: Vertebral body closest bony point to aorta            I: Aorta, closest point to vertebral body</p>	<p>Transverse cortical pedicle width (PW): Distance between point A and point B</p> <p>Distance to Dural Sac: Distance between point B and point C</p> <p>Chord length (CL): Distance between point D and point E</p> <p>Transverse pedicle angle (TPA): Angle produced by the lines DE and FG</p> <p>Distance to Aorta: Distance between point H and point I</p>
 <p>J: Left pedicle superior outer cortical margin            K: Left pedicle inferior outer cortical margin            L: Anterior cortical margin of the vertebral body in line with the left pedicle axis            M: Posterior cortical margin of the vertebral body in line with the left pedicle axis            N: Anterior aspect vertebral body in line with the vertebral endplates            O: Posterior aspect vertebral body in line with the vertebral endplates</p>	<p>Outer cortical margin pedicle height (PH): Distance between point J and point L</p> <p>Sagittal pedicle angle (SPA): Angle produced by the lines LM and NO</p>

Clinical scan images are presented such that left and right sides are shown in reverse

**Table 3** 95% Limits of agreement for intra- and inter-observer measurement variability

Measurement	Intra-observer error [mean ± 95% limits of agreement (1.96 × SD)]	Inter-observer error [mean ± 95% limits of agreement (1.96 × SD)]
Pedicle width (mm)	0.03 ± 0.91	0.25 ± 0.85
Distance to dural sac (mm)	0.09 ± 0.99	0.13 ± 1.83
Chord length (mm)	0.33 ± 2.28	1.27 ± 2.63
Distance to aorta (mm)	0.72 ± 4.01	0.31 ± 6.42
Pedicle height (mm)	− 0.15 ± 1.17	− 0.54 ± 1.23
Transverse pedicle angle (°)	− 0.09 ± 0.80	0.34 ± 1.96
Sagittal pedicle angle (°)	0.86 ± 5.99	0.19 ± 7.08

### Distance to dural sac

In the AIS patients, between the first and second scans, the distance from the left pedicle to the dural sac became significantly smaller at almost all levels ( $p < 0.05$  at T6, T8–10 and T12), while the distance from the right pedicle to the dural sac became longer at nearly all the levels, significantly so from the T5 to T10 ( $p < 0.05$ ). Comparatively, in the controls there were no significant differences found between the first and the second scans on either side of the vertebrae (Fig. 2).

### Distance to aorta

In the AIS scans, the distance to the aorta was significantly larger in the second scan at levels T6–T10 ( $p < 0.05$ ). There was no difference observed in the non-scoliotic control group between the two scans (Fig. 3). The change in distance

to the aorta was significantly correlated with patient height change ( $R^2 = 0.35$ ) and the Cobb angle change ( $R^2 = 0.22$ ) found between scans 1 and 2.

### Pedicle width

While the results suggest the pedicle width almost unanimously increased from scan 1 to 2, on both sides and in both groups, these were statistically significantly increased for AIS left pedicle of T12; control group left pedicles T5, T6 and T11; control group right pedicle T7 and T11 ( $p < 0.05$ ) (Fig. 4).

### Chord length

The chord length increased significantly from scan 1 to 2 in the AIS patients at levels T8, T9, T11 and T12 on the left side of the AIS curve ( $p < 0.05$ ) and was unchanged on the

**Fig. 2** Comparison between first and second scans showing the change in distance to dural sac from the left and right pedicles in AIS and non-scoliotic control subjects using MRI scans. Mean ± SD, \*denotes a statistically significant difference  $p < 0.05$ . A positive result implies an increase in distance to the dural sac between the first and second scans

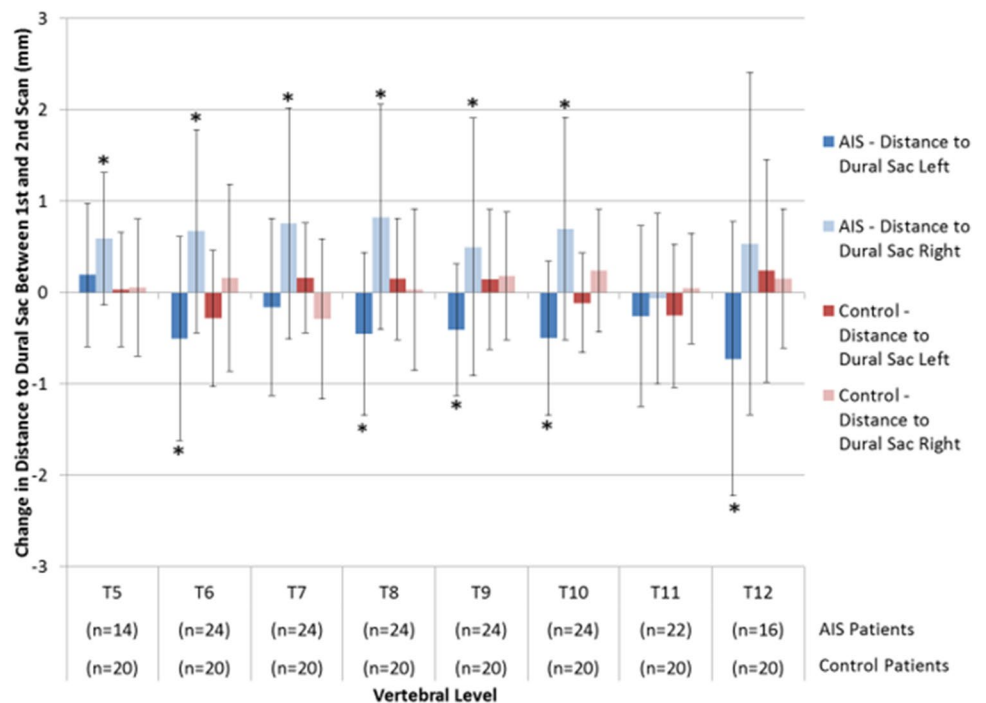


**Fig. 3** Comparison between the first and second scans showing the change in the distance to the aorta from the vertebrae in AIS and non-scoliotic control subjects using MRI scans. Mean  $\pm$  SD, \*denotes a statistically significant difference  $p < 0.05$ . A positive result implies an increase in the distance to aorta between the first and second scans

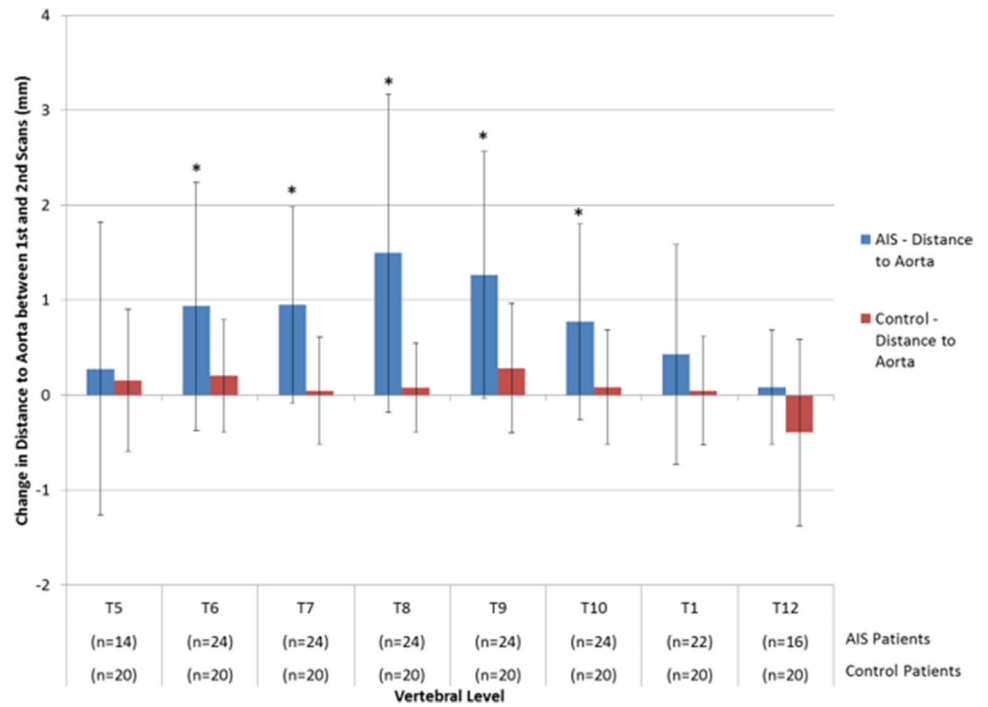
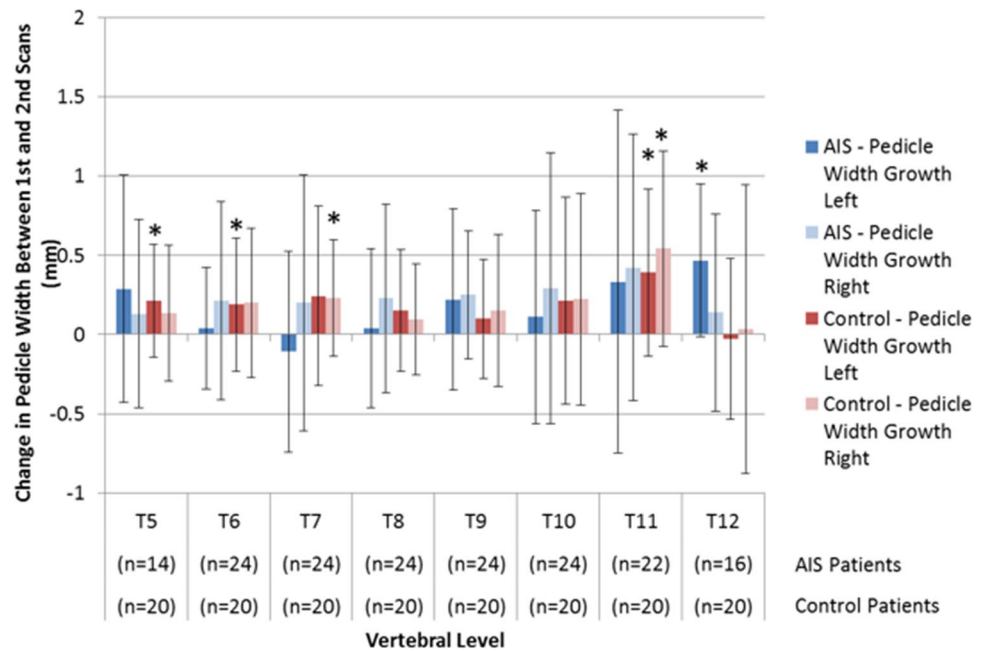


**Fig. 4** Comparison between the first and second scans showing left and right pedicle width growth in AIS and non-scoliotic control subjects using MRI scans. Mean  $\pm$  SD, \*denotes a statistically significant difference  $p < 0.05$ . A positive result implies an increase in pedicle width between the first and second scans



right. In the non-scoliotic group, there was no clear pattern or significant differences identified between the scans (Fig. 5).

**Transverse pedicle angle**

The TPA was noted to increase in size from scan 1 to 2 in the AIS group indicating a more posterolateral to

anteromedial trajectory of the pedicle at the levels of T8 and T9 on the left ( $p < 0.05$ ). In contrast, the right-sided TPA decreased significantly over time at T5, T6, T7 and T9 ( $p < 0.05$ ) indicating the pedicle trajectory became more parallel to the mid-sagittal line. In comparison, no significant changes were identified between scans in the control group (Fig. 6).

**Fig. 5** Comparison between the first and second scans showing left and right Chord length growth in AIS and non-scoliotic control subjects using MRI scans. Mean ± SD, \*denotes a statistically significant difference  $p < 0.05$ . A positive result implies an increase in chord length between the 1st and 2nd scans

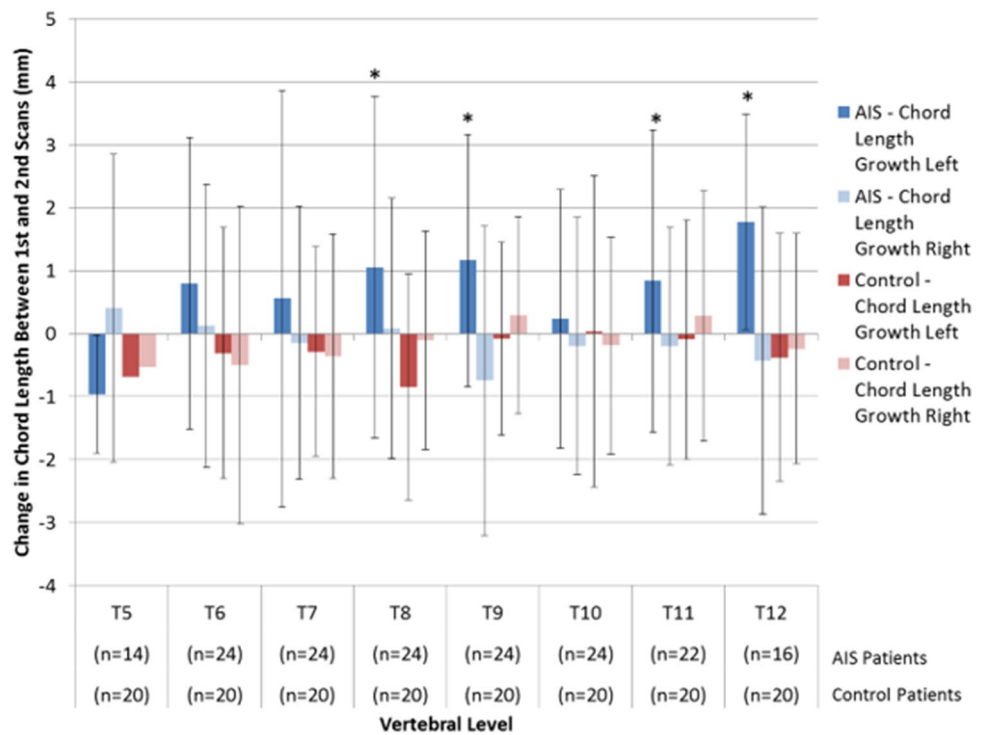
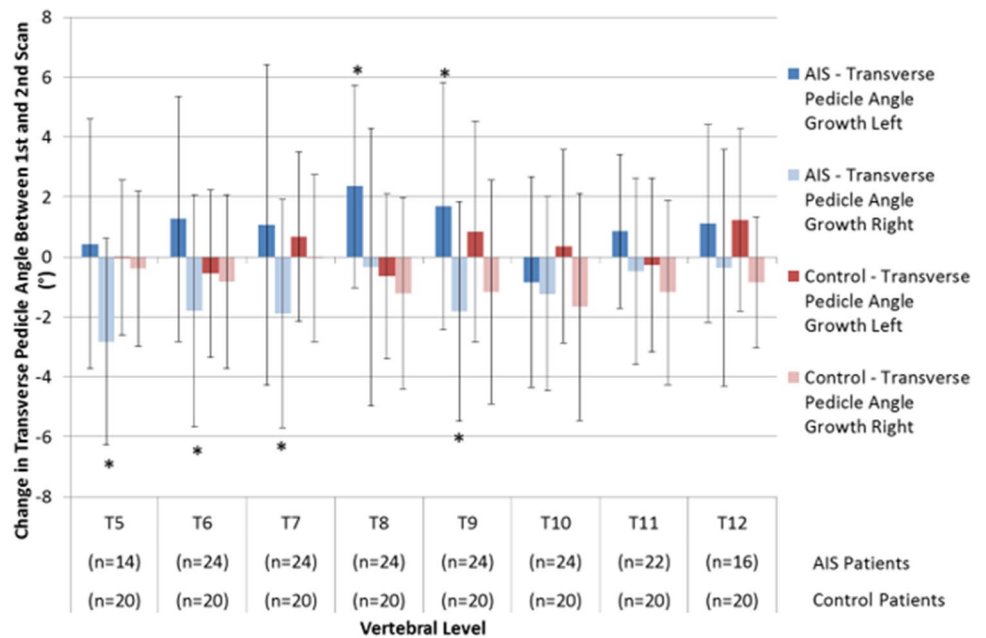


**Fig. 6** Comparison between the first and second scans showing left and right transverse pedicle angle growth in AIS and non-scoliotic control subjects using MRI scans. Mean ± SD, \*denotes a statistically significant difference  $p < 0.05$ . A positive result implies an increase in transverse pedicle angle between the first and second scans



**Pedicle height**

The mean pedicle height increased from scans 1 to 2 on both sides at all levels in both the AIS and control subjects (Fig. 7). For the control subjects, this increase was significant on each side and at every level ( $p < 0.05$ ). In AIS patients, significant increases were found at T6 and T8–12

inclusively on the left and all levels between T6 and T11 on the right ( $p < 0.05$ ).

When comparing asymmetric growth between the left and right sides of the curve, the pedicle height increase for the AIS group was greater on the right side between T6 and T9, and greater on the left at T11 and T12 ( $p < 0.05$ ).

**Fig. 7** Comparison between the first and second scans showing left and right pedicle height growth in AIS and non-scoliotic control subjects using MRI scans. Mean ± SD, \*denotes a statistically significant difference  $p < 0.05$ . A positive result implies an increase in pedicle height between the first and second scans

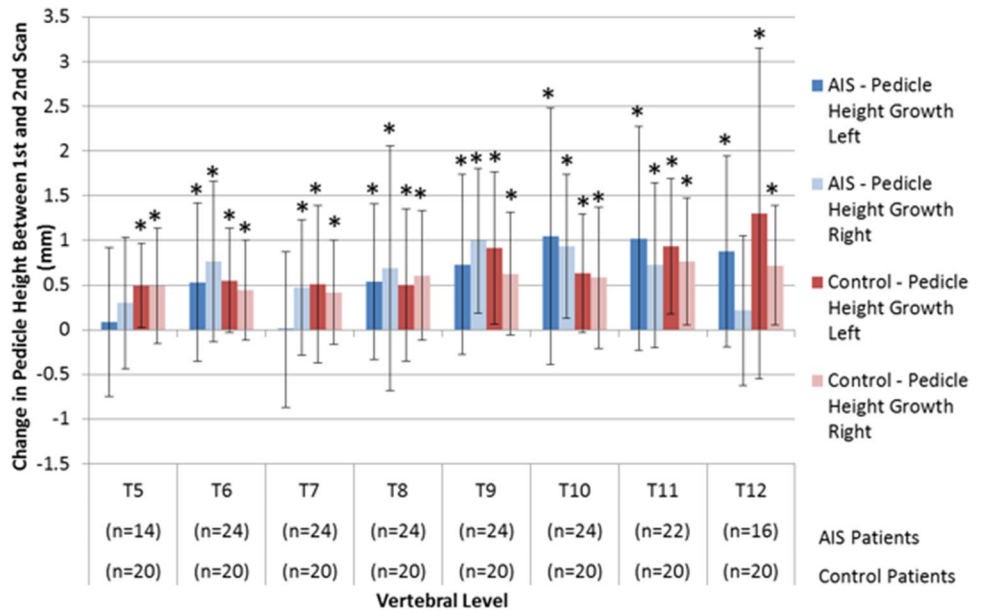
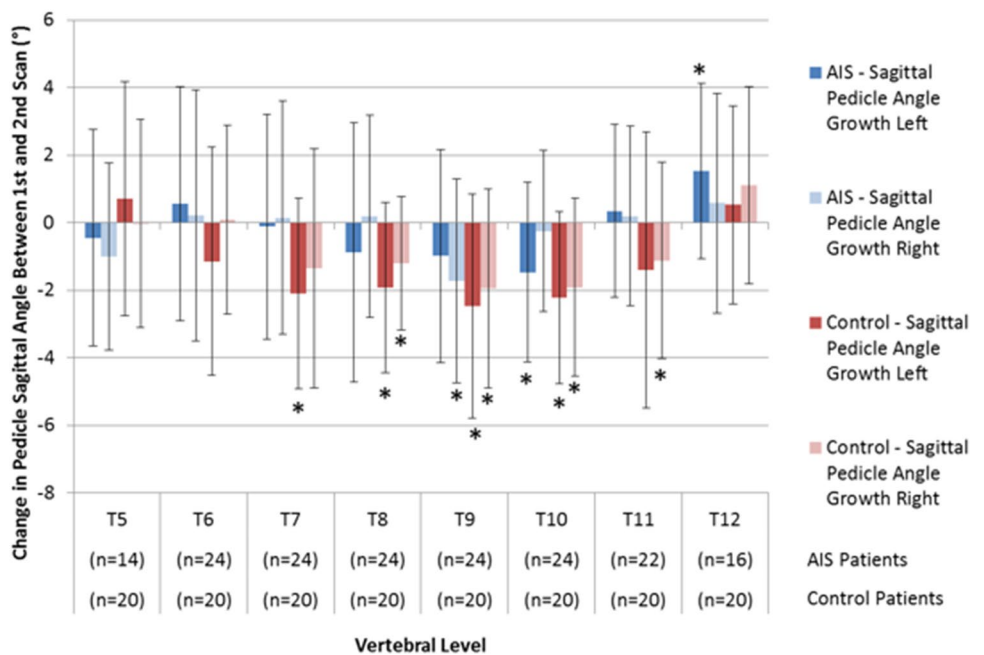


**Fig. 8** Comparison between the first and second scans showing left and right sagittal pedicle angle growth in AIS and non-scoliotic control subjects using MRI scans. Mean ± SD, \*denotes a statistically significant difference  $p < 0.05$ . A positive result implies an increase in sagittal pedicle angle between the first and second scans



**Sagittal pedicle angle**

SPA in the AIS group showed few significant changes between scans 1 and 2: left SPA decreased at T10 and increased at T12; right SPA decreased at T9 ( $p < 0.05$ ) (Fig. 8). In the non-scoliotic cohort, the SPA was significantly smaller at all levels from T7 to T10 on the left and from T8 to T11 on the right ( $p < 0.05$ ) indicating a more horizontal pedicle axis in the sagittal plane (Fig. 8).

**Regression analysis**

Change in standing height of the AIS group between scans 1 and 2 was positively correlated with the mean change in the pedicle height ( $R^2 = 0.6$ ) (Fig. 9) and pedicle width ( $R^2 = 0.2$ ). There was no correlation found between the change in major curve angle between scans and any of the pedicle morphology parameters (PW, CL, TPA, SPA) measured.



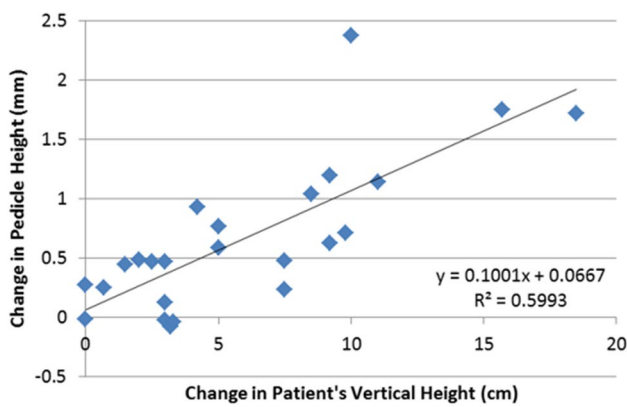


**Fig. 9** Change in pedicle height versus change in standing vertical height in AIS patients

In the non-scoliotic subjects, there was a weak correlation between the change in standing height between scans 1 and 2 and the mean change in pedicle height ( $R^2 = 0.2$ ), but no other correlations were identified between scans.

## Discussion

Understanding the changes that occur in the growing spine of AIS and non-scoliotic adolescents not only provides insight into the pathophysiology of AIS but provides data for the first time from a normal growing adolescent population with which to compare asymmetrical AIS growth. By selecting participants who are skeletally immature and at risk of major curve angle progression, this study was uniquely able to comprehensively evaluate the morphological evolution of individual vertebrae as the spine grew and the scoliosis progressed. This study also uniquely used MRI at repeated time points, which is the ideal medium to analyse the growing spine without exposing adolescents to any harmful ionising radiation.

Previous studies have analysed pedicle morphology of AIS patients at a single time point when the scoliotic curves had already reached operable severity [11, 19]. The current study demonstrated asymmetrical growth in AIS patients with larger pedicle height growth seen on the right (i.e. the convex side), longer chord length on the left and development of larger pedicle angles on the left, resulting in a more asymmetrical spine, findings that were not emulated in the non-scoliotic control subjects. Additionally, this study identified clear changes in the relationships of the aorta and dural sac with the vertebral margins as the scoliosis progressed with time and growth. The aorta became further away from the vertebrae around the apex of the curve as the scoliosis increased, which was not found in the control group with growth. In contrast, the dural sac migrated closer to the left

pedicle in the AIS patients while it remained midline in the non-scoliotic control subjects.

Accurately predicting curve progression is difficult, thus the AIS patients recruited to the study were more diverse compared to the control group with regards to age at the initial scan and, therefore, also the change in the vertical growth of the spine. Additionally, the progressive changes in AIS major curve angle were varied, with some patients demonstrating no clinical progression ( $< 5^\circ$ ) between the two scans.

The majority of the AIS patients (20/24) in this study were braced for a period during the study, which is the appropriate treatment for an immature female at risk of deformity progression. While the aim of bracing is to limit curve progression, it is uncertain whether bracing may have influenced the measured changes in major curve angle and/or pedicle morphology. Due to the varied patient compliance with brace wearing in the study and in general, this study was unable to ascertain a link between bracing and pedicle morphology development.

While only looking at bony pedicle canal dimensions, Sarwahi et al. [22] showed that MRI scans were similar to CT scans when classifying non-deformed pedicles. As MRI avoids exposing the subject to ionising radiation, it is the preferred imaging modality for paediatric and adolescent patient populations. Therefore, studies finding that MRI is an acceptable substitute for CT for imaging bony anatomy in the spinal column are of great interest. This current study showed that the intra- and inter-observer measurement reliability for MRI scans was superior in almost all measurements compared to a previous CT study [11] using the same measurement definitions, thereby providing evidence to support the utility of high-resolution 3D MRI for spinal bony anatomy measurements in the skeletally immature population.

While pedicle asymmetries in AIS patients are well documented [11, 14, 16, 19, 23–25], several studies have also shown vertebral asymmetry in non-scoliotic subjects [18, 26, 27]. The current study is unique in that it analyses the development of asymmetries over time, which can, therefore, identify and characterise progressive anatomical deformities. This provides new insights into the underlying pathophysiology of deformity progression as well as identifying novel targeted treatment options. Previous studies looking at pedicle development in AIS and non-AIS subjects have been limited to looking at different patient types at different stages and in the case of scoliosis patients, with different curve types analysed together [8, 16, 18, 26–31]. Rajwani et al., for example, compared 10 AIS patients with 8 control subjects with ages ranging from 1 to 15 years, finding asymmetries in both the control subjects and the AIS patients, and not unexpectedly no statistical differences between these two cohorts [27].

The more rapid chord length growth seen on the left side of the AIS curve in the current study is consistent with the expected deformity that develops whereby the vertebral body in the transverse plane veers towards the curve convexity in the spinal levels around the curve apex, as reported in previous studies [11, 17]. Similarly, the asymmetrical growth of AIS pedicle heights at T6–7 and the left-sided TPA becoming larger than the right was measured as it developed with curve progression in the current study, for the first time. Whether this asymmetry is from growth restriction on the concave side or excess growth on the convex side of the spine is uncertain. While pedicle height change and patient vertical standing height change correlated well in both non-scoliotic and AIS cohorts, no correlation was found between the change in Cobb angle and any of the pedicle morphology parameters which may have indicated a causative link. Given not all the scoliosis curves progressed, it was not expected that a definitive causal correlation could be found with the analysis. While the Liljenqvist et al. [19] study did not analyse deformity changes during spinal growth over time, it did also fail to find any correlation between pedicle asymmetry and Cobb angle in their cohort of preoperative AIS patients.

When considering the relationship between pedicle height and the sagittal pedicle angles together, it can be appreciated that over time, the pedicle height increases and the sagittal pedicle angle decreases (Figs. 7, 8). This translates to a more horizontal relationship between the vertebral body and the posteriorly attaching pedicles. While this could be due to an increase in the growth of the vertebral body when compared to the pedicle, it is postulated that this is as a result of the pedicle height growth occurring mainly from the inferior aspect of the pedicle. When specifically looking at the smaller pedicle height and larger pedicle angles near the concavity of the curve in AIS patients, one could hypothesise that there is growth restriction from the inferior aspect of these pedicles. Comparing these results with the vertebral body height changes in AIS patients during spinal growth over time would assist with further exploring this hypothesis.

The location of the dural sac, already skewed towards the concavity of the curve in scan 1, became even more skewed in the second scans; a finding not emulated in the non-scoliotic control subjects where the dural sac remained equidistant to the pedicles throughout the measured vertebrae in both scans. Clinically, this translates to a higher risk for neural injury from medial wall penetration as AIS patients mature and the scoliosis becomes larger. While previous reports have suggested epidural ‘safe zones’ of 2–3 mm [32] or 0–4 mm [33] medially in non-scoliotic spines and 0 mm in AIS patients [19], from analyses in the current study we recommend no medial wall penetration to reduce the potential risk of neural injury.

In contrast to the dural sac being more at risk from pedicle screw cortical breach medially, the aorta appears to be less at risk from a pedicle screw breach laterally as AIS curves increase in severity. As the right-sided curve increases, its distance to the midline and subsequently the left paraspinally placed aorta increases. While this study did not look specifically at the position of the aorta relative to other anatomical structures, it would be of interest to see whether the position of the aorta is affected as a result of the spinal curvature. Furthermore, looking at the location of the aorta in left sided curves would be of significant interest to surgeons. While the risk could be anticipated to be lower around the apex of the curve, it would be important to realise that in the upper and lower thoracic vertebrae at the limits of the curve in AIS patients, the aorta would be in close proximity to the vertebral body. It is also important to note that in the case of a left thoracic curve, neurovascular structures such as the azygous vein and visceral structures such as the pleura and lungs may be in close proximity to apical vertebral levels and potentially at risk of injury during surgical correction.

In addition to providing the above cautionary information for surgeons regarding pedicle screw placement in AIS correction surgery, this work has demonstrated the potential of high-resolution 3D MRI protocols to be the sole source of detailed patient-specific anatomical data to inform intra-operative monitoring systems and robotic-guided intervention procedures whilst avoiding radiation exposure to those benefiting from these technologies into the future.

## Conclusion

This study demonstrates for the first time the ability of sequential 3D MRI to analyse the changes in pedicle morphology and the relationships of neurovascular structures to vertebrae in AIS patients over time and additionally compares these changes to the changes seen in non-scoliotic subjects during growth. The measurement reliability for MRI scans was superior in almost all measurements compared to a previous CT study using the same measurement definitions, thereby providing evidence to support the utility of high-resolution 3D MRI for spinal bony anatomy measurements in the skeletally immature population, without using ionising radiation. These findings enhance our understanding of the pedicle morphology and growth in the immature spine as well as in AIS patients, and its relationship to key neurovascular structures and are useful both in understanding the natural history of AIS as well as in assisting safe pedicle screw placement during scoliosis correction surgery using a posterior approach.

## Key points

- Sequential MRI scans at approximately 1 year apart provide new information on how the posterior elements become asymmetrical with curve progression in adolescent idiopathic scoliosis versus adolescents without scoliosis.
- MRI is the ideal method to study the growing spine as it does not expose children and adolescents to ionising radiation.
- During scoliosis progression of right-sided main thoracic curves, the dural sac becomes closer to the left apical pedicles and the distance from the apical vertebrae to the aorta becomes larger.
- The mean pedicle height increased significantly from MRI 1 to MRI 2 at all levels symmetrically in the non-scoliotic subjects but was significantly asymmetric around the apex of the scoliosis with right pedicle heights increasing more than left.

**Acknowledgements** We wish to pay tribute to a valued member of our Spine Research Group, Associate Professor Clayton James Adam who passed away before this manuscript was completed and will be forever missed by the QUT team.

**Author contributions** CMD: conceptualisation, data acquisition, data analysis and interpretation, and drafting and revision of manuscript and approval of final manuscript; CAG: conceptualisation, investigation design, data analysis and interpretation, critical revision for intellectual content of manuscript and approval of final manuscript; MTI: conceptualisation, data acquisition, critical revision for intellectual content of manuscript and approval of final manuscript; GNA: conceptualisation, data acquisition, critical revision for intellectual content of manuscript and approval of final manuscript; RDL: conceptualisation, data acquisition, critical revision for intellectual content of manuscript and approval of final manuscript; Clayton J. Adam (deceased): substantial contribution to conceptualisation, investigation design, data analysis and interpretation, and critical revision for intellectual content of early manuscript draft versions; MJP: conceptualisation, investigation design, data analysis and interpretation, critical revision for intellectual content of manuscript and approval of final manuscript; JPL: conceptualisation, investigation design, data analysis and interpretation, critical revision for intellectual content of manuscript and approval of final manuscript.

**Funding** No funds were received in support of this work. Partial postgraduate scholarship funding for the first author was provided by Queensland X-Ray Ltd (Australia) and Children's Health Queensland, Australia.

## Compliance with ethical standards

**Conflict of interest** The authors declare they have no conflict of interest.

**Ethics approvals** Ethical approvals were obtained from Mater Human Research Ethics Committee (HREC) 14/88/AM03, the Queensland University of Technology HREC (1200000281) and the Children's

Health Queensland HREC (14/QRCH/411). The authors certify that the study was performed in accordance with the ethical standards as laid down in the 1064 Declaration of Helsinki and its later amendments.

**Informed consent** Written informed consent was obtained from all participants and their parent or legal guardian.

## References

1. Kane WJ (1977) Scoliosis prevalence: a call for a statement of terms. *Clin Orthop Relat Res* 126:43–46
2. Kim H, Kim HS, Moon ES, Yoon CS, Chung TS, Song HT et al (2010) Scoliosis imaging: what radiologists should know. *Radiographics* 30(7):1823–1842
3. Weinstein SL, Dolan LA (2015) The evidence base for the prognosis and treatment of adolescent idiopathic scoliosis: the 2015 orthopaedic research and education foundation clinical research award. *J Bone Jt Surg Am* 97(22):1899–1903
4. Justice CM, Miller NH, Marosy B, Zhang J, Wilson AF (2003) Familial idiopathic scoliosis: evidence of an X-linked susceptibility locus. *Spine (Phila Pa 1976)* 28(6):589–594
5. Hu X, Siemionow KB, Lieberman IH (2014) Thoracic and lumbar vertebrae morphology in Lenke type 1 female adolescent idiopathic scoliosis patients. *Int J Spine Surg* 8
6. Jutte PC, Castelein RM (2002) Complications of pedicle screws in lumbar and lumbosacral fusions in 105 consecutive primary operations. *Eur Spine J* 11(6):594–598
7. Kosmopoulos V, Schizas C (2007) Pedicle screw placement accuracy: a meta-analysis. *Spine (Phila Pa 1976)* 32(3):E111–E120
8. Taylor JR (1983) Scoliosis and growth. Patterns of asymmetry in normal vertebral growth. *Acta Orthop Scand* 54(4):596–602
9. Tian NF, Huang QS, Zhou P, Zhou Y, Wu RK, Lou Y et al (2011) Pedicle screw insertion accuracy with different assisted methods: a systematic review and meta-analysis of comparative studies. *Eur Spine J* 20(6):846–859
10. Vaccaro AR, Rizzolo SJ, Balderston RA, Allardyce TJ, Garfin SR, Dolinskas C et al (1995) Placement of pedicle screws in the thoracic spine. Part II: An anatomical and radiographic assessment. *J Bone Jt Surg Am* 77(8):1200–1206
11. Davis CM, Grant CA, Pearcy MJ, Askin GN, Labrom RD, Izatt MT et al (2017) Is there asymmetry between the concave and convex pedicles in adolescent idiopathic scoliosis? A CT investigation. *Clin Orthop Relat Res* 475(3):884–893
12. Liljenqvist UR, Link TM, Halm HF (2000) Morphometric analysis of thoracic and lumbar vertebrae in idiopathic scoliosis. *Spine (Phila Pa 1976)* 25(10):1247–1253
13. Smith RM, Pool RD, Butt WP, Dickson RA (1991) The transverse plane deformity of structural scoliosis. *Spine (Phila Pa 1976)* 16(9):1126–1129
14. Upendra B, Meena D, Kandwal P, Ahmed A, Chowdhury B, Jayaswal A (2010) Pedicle morphometry in patients with adolescent idiopathic scoliosis. *Indian J Orthop* 44(2):169–176
15. Vaccaro AR, Rizzolo SJ, Allardyce TJ, Ramsey M, Salvo J, Balderston RA et al (1995) Placement of pedicle screws in the thoracic spine. Part I: Morphometric analysis of the thoracic vertebrae. *J Bone Jt Surg Am* 77(8):1193–1199
16. Xiong B, Sevastik B, Willers U, Sevastik J, Hedlund R (1995) Structural vertebral changes in the horizontal plane in idiopathic scoliosis and the long-term corrective effect of spine instrumentation. *Eur Spine J* 4(1):11–14
17. Zindrick MR, Wiltse LL, Doornik A, Widell EH, Knight GW, Patwardhan AG et al (1987) Analysis of the morphometric

- characteristics of the thoracic and lumbar pedicles. *Spine (Phila Pa 1976)* 12(2):160–166
18. Sarwahi V, Sugarman EP, Wollowick AL, Amaral TD, Lo Y, Thornhill B (2014) Prevalence, distribution, and surgical relevance of abnormal pedicles in spines with adolescent idiopathic scoliosis vs. no deformity: a CT-based study. *J Bone Jt Surg Am* 96(11):e92
  19. Liljenqvist UR, Allkemper T, Hackenberg L, Link TM, Steinbeck J, Halm HF (2002) Analysis of vertebral morphology in idiopathic scoliosis with use of magnetic resonance imaging and multiplanar reconstruction. *J Bone Jt Surg Am* 84-A(3):359–368
  20. Risser JC (2010) The classic: The iliac apophysis: an invaluable sign in the management of scoliosis. Reprint of 1958 article. *Clin Orthop Relat Res* 468:646–653
  21. Bland JM, Altman DG (2003) Applying the right statistics: analyses of measurement studies. *Ultrasound Obstet Gynecol* 22(1):85–93
  22. Sarwahi V, Amaral T, Wendolowski S, Gecelter R, Sugarman E, Lo Y et al (2016) MRIs are less accurate tools for the most critically worrisome pedicles compared to CT scans. *Spine Deform* 4(6):400–406
  23. Abul-Kasim K, Ohlin A (2012) Patients with adolescent idiopathic scoliosis of Lenke type-1 curve exhibit specific pedicle width pattern. *Eur Spine J* 21(1):57–63
  24. Catan H, Buluc L, Anik Y, Ayyildiz E, Sarlak AY (2007) Pedicle morphology of the thoracic spine in preadolescent idiopathic scoliosis: magnetic resonance supported analysis. *Eur Spine J* 16(8):1203–1208
  25. O'Brien MF, Lenke LG, Mardjetko S, Lowe TG, Kong Y, Eck K et al (2000) Pedicle morphology in thoracic adolescent idiopathic scoliosis: is pedicle fixation an anatomically viable technique? *Spine* 25(18):2285–2293
  26. Peters JR, Chandrasekaran C, Robinson LF, Servaes SE, Campbell RM Jr, Balasubramanian S (2015) Age- and gender-related changes in pediatric thoracic vertebral morphology. *Spine J* 15(5):1000–1020
  27. Rajwani T, Bagnall KM, Lambert R, Videman T, Kautz J, Moreau M et al (2004) Using magnetic resonance imaging to characterize pedicle asymmetry in both normal patients and patients with adolescent idiopathic scoliosis. *Spine (Phila Pa 1976)* 29(7):E145–E152
  28. Hassan E, Liau KM, Ariffin I, Halim YA (2010) Internal morphometry of thoracic pedicles in the immature spine. *Spine (Phila Pa 1976)* 35(13):1253–1256
  29. Liu J, Shen J, Zhang J, Li S, Zhao H, Qiu G et al (2012) The position of the aorta relative to the spine for pedicle screw placement in the correction of idiopathic scoliosis. *J Spinal Disord Tech* 25(4):E103–E107
  30. Morales-Avalos R, Leyva-Villegas J, Sanchez-Mejorada G, Cardenas-Serna M, Vilchez-Cavazos F, Martinez-Ponce De Leon A et al (2014) Age- and gender-related variations in morphometric characteristics of thoracic spine pedicle: a study of 4800 pedicles. *Clin Anat* 27(3):441–450
  31. Shaikh KA, Bennett GM, White IK, Bullis CL, Fulkerson DH (2012) Computed-tomography-based anatomical study to assess feasibility of pedicle screw placement in the lumbar and lower thoracic pediatric spine. *Childs Nerv Syst* 28(10):1743–1754
  32. Roy-Camille R, Saillant G, Mazel C (1986) Internal fixation of the lumbar spine with pedicle screw plating. *Clin Orthop Relat Res* 203:7–17
  33. Gertzbein SD, Robbins SE (1990) Accuracy of pedicular screw placement in vivo. *Spine (Phila Pa 1976)* 15(1):11–14

**Publisher's Note** Springer Nature remains neutral with regard to jurisdictional claims in published maps and institutional affiliations.